Fab & Facilities

Materials

Cell Processing

Thin Film

PV Modules

Power Generation

# Improvements in advanced industrial n-type solar cells and modules

Ingrid Romijn, Bas van Aken, John Anker, Ian Bennet, Bart Geerligs, Nicolas Guillevin, Astrid Gutjahr, Eric Kossen, Martien Koppes & Kees Tool, ECN Solar Energy, Petten, Marten Renes & Peter Venema, Tempress Systems BV, Vaassen, & Nico van Ommen & Jan Bakker, Eurotron BV, Bleskensgraaf, The Netherlands

### **ABSTRACT**

This paper reports on the progress of R&D in two n-type cell and module concepts: the n-Pasha solar cell and bifacial module, and the n-MWT (metal wrap-through) cell and module. Both are part of ECN's technology platform, acting as a roadmap for research in n-type Cz cells and modules. The technology platform also encompasses low-cost IBC solar cells. In the case of n-Pasha, recent developments involve improved stencil-printed metallization, resulting in an increased  $I_{\rm sc}$  and  $V_{\rm oc}$  and efficiencies of up to 20.5%. For the bifacial module aspect, research has been done on the effect of different albedo on the module output. A gain of  $20\%_{\rm rel}$  in module output power was obtained with an optimized background, increasing the module power from 314W to 376W. As regards n-MWT cells, the front-side metallization pattern has been changed significantly. The number of vias for conducting the emitter current to the rear has been increased from 16 to 36, resulting in reduced lengths of busbars and fingers and consequently an increase in FF. At the same time, the metal coverage on the front side has been reduced from 5% to 3% of the total area, leading to a gain in  $I_{\rm sc}$  and  $V_{\rm oc}$  and a significant reduction in Ag consumption. All these factors will result in a lower cost/Wp. For the improved n-MWT design, average efficiencies of 20.8% over a large batch (134) of cells have been obtained, with the highest recorded efficiencies being 21.0%.

### **Introduction: n-type cell concepts**

High efficiency, ease of industrialization and reliability are the main drivers towards low-cost (€/Wp) silicon PV. The March 2014 edition of

the International Technology Roadmap for PV (ITRPV) envisages the share of n-type solar cells and modules becoming close to 40% in the next 10 years [1]. Compared with p-type material, n-type Cz material is known for its stable high carrier lifetimes because of the absence of light-induced degradation (LID) [2] and its higher tolerance to the most common metallic impurities such as Fe [3]. These longer lifetimes are consequently reflected in

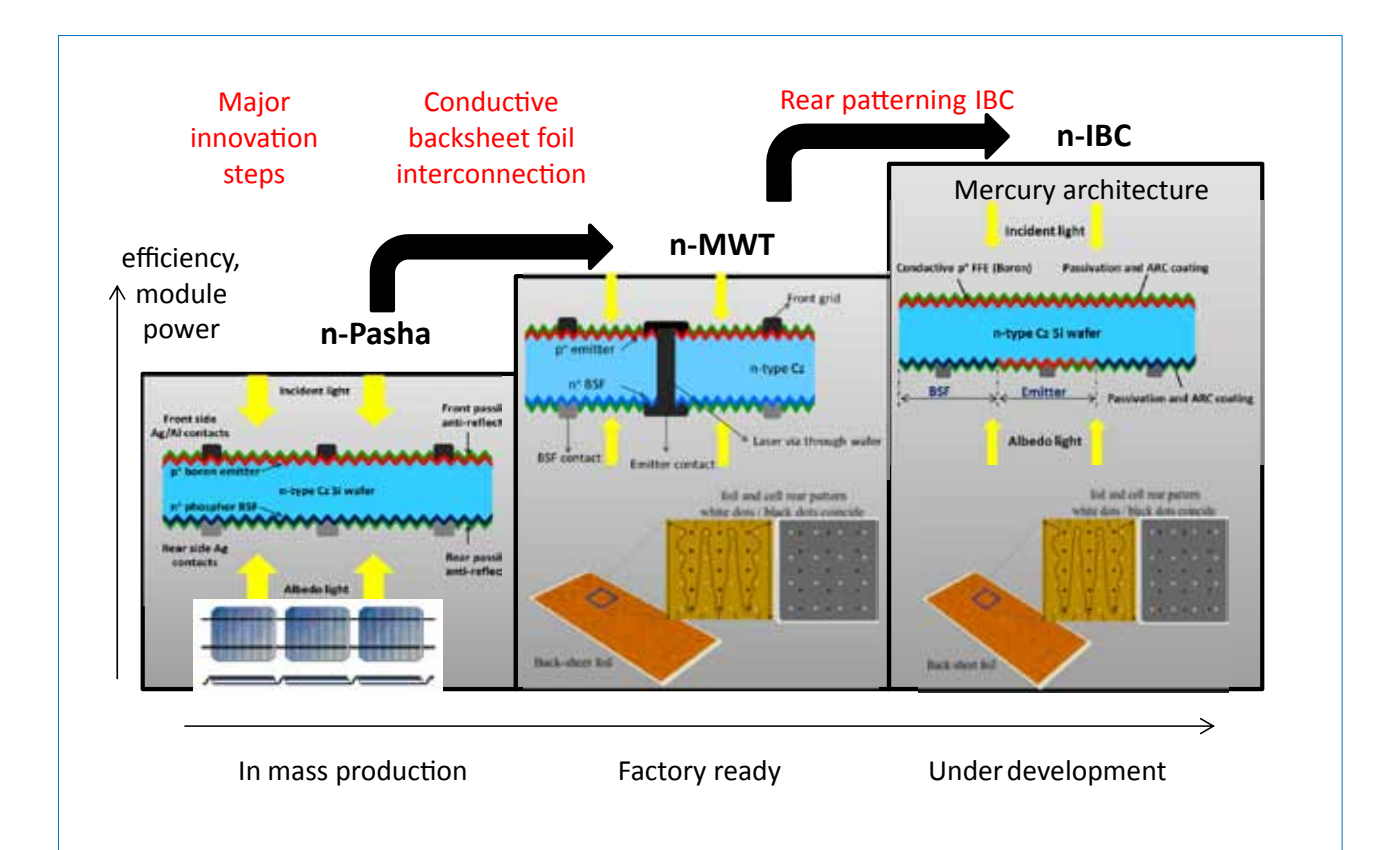


Figure 1. ECN's technology platform for cells and modules on n-type Cz material. It encompasses three technologies that are logical steps on the efficiency and development ladder.

higher efficiencies; indeed, the highest efficiency crystalline silicon modules currently on the market are based on the SunPower Maxeon technology, which uses n-type Cz material for manufacturing interdigitated back-contact (IBC) solar cells with efficiencies above 24%, and module efficiencies above 21% [4]. Very high efficiencies on n-Cz material can also be obtained with the heterojunction (HIT) technique used by Panasonic; Panasonic recently reported cell efficiencies of 25.6%, made possible by combining heterojunction and backcontact (IBC) technologies [5].

"The March 2014 edition of the ITRPV envisages the share of n-type solar cells and modules becoming close to 40% in the next 10 years."

Many institutes and companies have started to adopt simpler structures on n-type Cz material that still enable efficiencies above 20% to be realised. Yingli Solar began mass production of their PANDA cell line in 2010, and in 2012 was already reporting efficiencies of 20% [6]. Other companies, such as PVGS [7] and Motech [8], are now also reporting efficiencies of 20–20.5% for bifacial n-type cells from their R&D or pilot production using boron emitter diffusion. Others, like Bosch [9] and CEA/INES [10], adopt ion implantation for the back-surface field (BSF) and

emitter formation, which yields efficiencies higher than 20.5%. Recently, FhG ISE has taken a different approach to obtaining higher efficiencies by using (on a laboratory scale) passivated rear contacts and a selective emitter in their TopCon process, enabling an efficiency of 24.4% to be achieved [11].

### ECN's n-type technology platform

ECN's aim is to develop highly efficient, low-cost and reliable solar cell and module concepts that can be easily adopted in mainstream industrial production. On the basis of over 10 years of research, ECN has established a technology platform on n-type Cz material that encompasses three different cell-module concepts (see Fig. 1). The basis of the technology platform is the relatively simple n-Pasha cell [12] - a bifacial solar cell with H-patterned metallization on both front and rear. ECN, Tempress and Yingli introduced this cell to the market in 2010 as a novel bifacial cell concept called PANDA [13], while in 2013 Nexolon America selected this cell concept for their new production line, enabling the production of bifacial modules.

The next step up in performance on the technology platform is the back-contact n-MWT (metal wrap-through) integrated cell and module concept, which combines two of ECN's cell concepts that are already proven both in the laboratory and on a large scale in industry: 1) ECN's p-type MWT cell and module concept [14], based on foil

interconnection; and 2) the n-Pasha n-type cell concept, as described above. The n-MWT cell process is very close to that of the n-Pasha cell, while yielding a higher short-circuit current and corresponding efficiency because of the reduction in front-side metal coverage [15]. The modules are produced using a conducting backsheet foil, on which the cells are assembled with conductive adhesive. The back-contact foil technology enables higher module power as a result of the reduction in cell-tomodule losses, because relatively wide metal grids in the conducting foil can be used and connected to many contact spots on the rear side of the cells. The n-MWT modules are ready to be produced on an industrial scale, as Yingli announced recently in a press release [16].

Apart from being a cost-effective high-efficiency PV technology, n-MWT technology is also a bridge or a step in the roadmap from n-Pasha to n-type IBC technology. In an IBC cell, the p-n junction and all metallization is moved to the rear. Recently ECN presented n-type IBC Mercury cells [17], which employ a relatively conductive front floating emitter to avoid electrical shading issues present in conventional front-surface field (FSF) IBC cells, resulting in relaxed demands on the geometrical resolution in the processing. This allows the processing of highly efficient solar cells (no metal on the front side) with a process complexity similar to that for n-pasha and n-MWT cells. The IBC Mercury design can be combined with

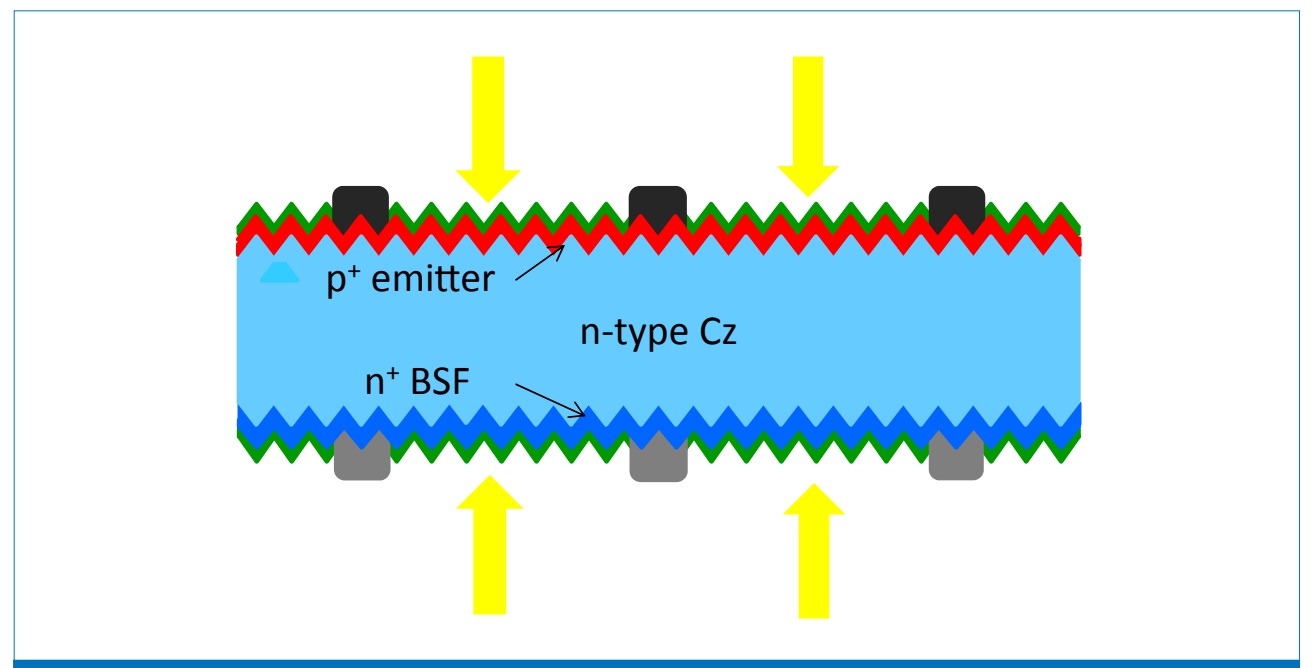


Figure 2. Cross section of the ECN n-Pasha cell, featuring an n-type Cz Si wafer with a boron  $p^+$  emitter and a phosphorus  $n^+$  BSF. Yingli's PANDA cells are also based on this structure.

back-contact module technology in a very similar way to n-MWT modules.

This paper will focus on the first two concepts of the technology platform: the n-Pasha cell and bifacial module, and the n-MWT cell and foilinterconnection module.

### The n-Pasha cell

The basic configuration of the n-Pasha solar cell is shown in Fig. 2. The n-Pasha cells are fabricated on 6-inch n-type Cz wafers, and all processing steps used are compatible with an industrial-scale production. The texturing and cleaning steps are performed by wet chemical processes, while both the  $p^+$  (boron) and  $n^+$ (phosphorus) doped layers are created by tube furnace diffusion processes. Passivation and anti-reflection coatings are deposited using plasmaenhanced chemical vapour deposition (PECVD) tools. The metal grids are printed, and the contacts on the emitter and BSF are formed during a single co-firing step. Both front and rear metallization can be directly soldered, so no additional metallization step is necessary to enable cell interconnection into a module. The n-Pasha solar cells fabricated using the ECN 'baseline' process now typically achieve average efficiencies above 20% on a wide range of materials. The consistent performance of n-Pasha processing for different materials and a wide range of base resistivities was extensively tested and published in 2013 [18]. More details regarding n-Pasha cell processing can be found in previous publications [12,13,18].

If the n-Pasha cells are assembled in a standard monofacial module, maximum light trapping can be obtained by the rear dielectric layers in combination with a reflecting backsheet foil. On the other hand, the open rear-side H-patterned metallization makes the n-Pasha concept very suitable for bifacial cell and module technology, in which case

an even higher module output power and an increased annual energy yield can be obtained when the modules are appropriately placed in the field.

### Bifacial n-Pasha modules

Because of the transparent rear side and the absorbent background, bifacial modules demonstrate lower efficiency or power output per unit area when measured under standard test conditions (STC) than monofacial modules. However, the annual output of bifacial modules can be significantly higher, depending on albedo, orientation and tilt angle [19-21]. At ECN, 72-cell bifacial modules were manufactured using six 12-cell strings made of (relatively old) n-Pasha solar cells with efficiencies of 19.0%. A resulting peak power of 314W was measured for the bifacial module under STC of 1000W/m<sup>2</sup> irradiation,

 $25^{\circ}$ C and a black background and environment. With another batch of n-Pasha cells of 19.6% efficiency, a monofacial 72-cell module was made that produced 334W. Average cell and corresponding module I-V data are summarized in Table 1, together with the cell-to-module (CtM) ratios for the bifacial and monofacial modules. The modules were measured under STC, which includes an absorbent black background.

The CtM ratios for  $V_{\rm oc}$  (above 100%) and FF (above 96%) are very similar for both modules. The  $I_{\rm sc}$  CtM ratio for the bifacial modules, however, is 2.7% lower (99.7% compared with 102.4%): this difference can be directly related to the loss of transmitted light that is not reflected at the white backsheet but absorbed in the black background.

To simulate the effect of albedo on the power output of bifacial modules, and evaluate the potential gain for

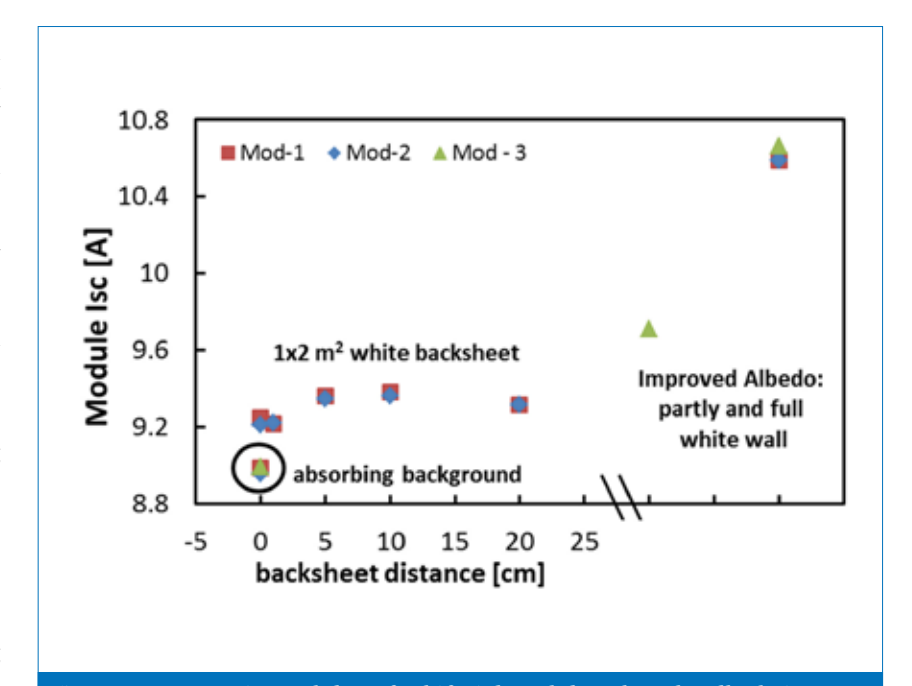


Figure 3. Increase in module  $I_{\rm sc}$  for bifacial modules when the albedo is changed. Under STC with an absorbent background, the  $I_{\rm sc}$  for all modules is under 9A; with a full white wall behind the module, the  $I_{\rm sc}$  becomes 10.6A, with a corresponding module output of 376W.

Module		<i>I</i> <sub>sc</sub> [A]	<i>V</i> <sub>oc</sub> [V]	FF [-]	Eta [%]	$P_{\text{max}}[W]$
Bifacial with ARC	Avg cell	9.14	0.638	78.0	19.05	4.55
	72-cell module	9.12	45.98	75.0	18.3 (per cell)	314.3
	CtM ratio	99.7%	100.1%	96.2%	96.0%	
	Full white wall	10.59				376
Monofacial with ARC	Avg cell	9.25	0.650	77.9	19.6	4.69
	72-cell module	9.47	47.16	74.9	19.5 (per cell)	334.4
	CtM ratio	102.4%	100.7%	96.1%	99.1%	

Table 1. Cell and module data for bifacial and monofacial modules manufactured from n-Pasha cells, measured under STC (and also with a full white wall behind the bifacial module).

Finger width [µm]	<i>I</i> <sub>sc</sub> [A]	$J_{ m sc}$ [mA/cm $^2$ ]	<i>V</i> <sub>oc</sub> [V]	FF [-]	Eta [%]
55 avg	9.29	38.87	0.649	78.89	19.9
45 avg	9.44	39.49	0.651	78.15	20.1
40 avg	9.45	39.54	0.654	78.49	20.3 (20.5 max)

Table 2. Average I-V data for n-Pasha cells with different front metallization: the finger width of the stencilled fingers is decreased while the number of fingers stays the same.

the bifacial modules when they are placed in a proper environment, two bifacial modules were measured with a white backsheet (same material as for the monofacial module) at various distances behind the module (see Fig. 3). With a white backsheet directly against the transparent backsheet, the  $I_{\rm sc}$  of the bifacial module increased to the value expected for the same module in a monofacial layout, namely 9.2A. When the white backsheet was placed further away from the module (5 to 20cm), the  $I_{\rm sc}$  output increased even more. A full white back wall (approximately  $3m \times 2m$ , behind the module) yielded 10.6A and 376W; more than 90% of the gain is due to rear illumination.

In summary, when bifacial n-Pasha modules are placed in an environment with sufficient albedo (for instance crushed shells or specially coated roofs, so-called *cool roofs*), a gain in

module output power of up to 20% (314W to 376W) is observed.

"When bifacial n-Pasha modules are placed in an environment with sufficient albedo, a gain in module output power of up to 20% is observed"

## Improvements in n-Pasha cell and module: metallization

To reduce Ag consumption, increase the active area of the cell, and decrease recombination losses due to the metallization grid, stencil printing of narrow high-aspect-ratio lines was investigated. An added advantage of stencil printing is the uniformity of the print cross section, improving the efficiency of the Ag usage. The results are presented here for three different stencil designs with nominally 40-, 45- and 55µm-wide fingers. All other processing, including the number of grid fingers, was kept constant. The resulting average cell parameters are shown in Table 2. For the best cell group, average efficiencies of 20.3% and a highest efficiency of 20.5% were obtained. The gain in  $I_{sc}$  for the 45and 40µm-wide fingers is even larger than expected for the decreased finger width: this may be due to the change of metal paste for these two groups, which enabled fingers with very high aspect ratios of almost 1, and is currently under investigation.

These cells were subsequently laminated in single-cell test laminates using a white backsheet similar to the monofacial module in Table 1. The



# Levitrack ALD for Mass-Production

### **Applications**

- Passivation by ALD Aluminium Oxide
- Multi-crystalline silicon cells
- Mono-crystalline silicon cells
- p-Type silicon cells
- n-Type silicon cells

### **Features**

- Single side deposition
- High throughput; >3,000wph guaranteed
- Contactless transport during processing
- Rapid and inline wafer heat-up and cool-down
- Efficient TMA usage; >25%
- Operation under atmospheric conditions; no vacuum pumps



module  $I_{\rm sc}$  increases in all cases, as compared with the cell  $I_{\rm sc}$ . The CtM ratio gain in  $I_{\rm sc}$  is somewhat lower for the narrow-finger cells, as can be expected from the reduced benefit from the internal reflection of light scattered off the fingers inside the module. Very high currents of up to 9.6A were

measured for the best single-cell laminates, as shown in Fig. 4.

### Improvements in bifacial module: Bumblebi

Typical bifacial modules do not have an equal power (or appearance) on both sides of the module, mainly because of the lower  $I_{\rm sc}$  when the modules are illuminated from the rear. A new approach in which the front and rear response (and appearance) of the modules is equalized is currently under investigation at ECN and will be briefly described in this section. An equal front and rear response of a module will be especially useful if the bifacial modules are used in an east—west orientation, because in this case the harvested power will be more evenly distributed over the whole day.

In this new approach, named Bumblebi, 50% of the cells in a module are turned around: thus each side of the module has 50% of the cells with the positive contact(s) and 50% of the cells with the negative contacts on that side. To avoid the current mismatch between turned cells, the forward- and backward-facing cells are connected in series in separate strings, which are subsequently connected in parallel (ECN patent pending). The idea is shown in Fig. 5 for small 2×2 modules, but this can easily be extrapolated to larger strings, e.g. 60or 72-cell modules. The first results from these mini-modules indicate that the Bumblebi module outperforms by ~3%<sub>rel</sub> the regular bifacial geometry under bifacial circumstances (diffuse light and addition of white panels as a back wall in the Pasan flash tester). The improved performance is confirmed by modelling and further experimental investigation is currently under way.

## 9.7 9.6 9.5 9.4 9.3 9.2 9.1 40 45 Finger width [μm]

Figure 4. Improvement in  $I_{\rm sc}$  for mini-modules made from four cells, for different front-finger widths.

# 

Figure 5. Schematic view of a normal bifacial, a mixed-cell bifacial and a Bumblebi bifacial mini-module. F and R indicate the front and rear sides of the bifacial n-Pasha cells. Module 1 has no mismatch but is asymmetric in terms of front and rear illumination. The second module has mismatch in  $I_{\rm sc}$  because of the mixing of F and R cells, but is symmetric in front and rear illumination. Module 3, the Bumblebi, has a very small voltage mismatch because of F and R strings, but is also symmetric.

### n-MWT cells

The n-MWT cell processing in general remains very close to the conventional front-to-back contact n-Pasha cell processing. Additional laser processing is used to form via holes by means of which the front-side metal grid is wrapped through the wafer. Like the n-Pasha cells, the cell structure comprises a front-side boron emitter, a phosphorus BSF and an open rearside metallization suitable for thin wafers (Fig. 6). Metal contacts can be deposited by an industrial screenprinting process with no further requirements regarding alignment compared with the screen-printing process used in the industrial n-Pasha process. The front- and rear-side metal grid patterns can be based on a H-pattern lookalike grid design, or on a modular (front) grid design, combined with the unit cell concept.

To compare the performance of n-MWT with n-Pasha cells, both cell types were prepared from adjacent n-type Cz wafers (239cm², 200µm

Cell	
Proc	essing

	$J_{ m sc}$ [mA/cm $^2$ ]	<i>V</i> <sub>oc</sub> [V]	FF [-]	Eta [%]	$R_{\rm series}$ [m $\Omega$ ]
n-Pasha avg	38.90	652	78.4	19.89	4.9
n-Pasha best	38.97	653	78.5	19.98	4.8
n-MWT avg	39.95	652	76.8	20.04	5.7
n-MWT best	40.01	653	77.0	20.10	5.6

Table 3. I-V characteristics of n-Pasha and n-MWT cells with comparable  $J_0$  and metallization parameters. ( $R_{\text{series}}$  was obtained from the fit to a two-diode model.)

thickness, approximately  $1.7\Omega\cdot cm$  resistivity). Both groups were processed in parallel and received comparable processing, with the exception of the steps specific to n-MWT, such as via drilling and via metallization. The I-V data are presented in Table 3: average efficiencies of 20.04 and 19.89% respectively were obtained for n-MWT and n-Pasha, equating to a  $0.15\%_{abs}$  efficiency gain for n-MWT over n-Pasha [15].

The  $J_{\rm sc}$  gain of 2.6% for the n-MWT cells is related to the reduced front metal-shading losses thanks to the narrow and tapered front busbars. Because the n-Pasha process used non-contacting front busbar paste [18], there is no additional  $V_{\rm oc}$ gain realized by the n-MWT cells from the reduction of busbar area (reduced metal recombination). In this experiment the cell efficiency benefit of the MWT structure is therefore  ${\sim}0.15\%_{abs}\text{, compared with}$  ${\sim}0.25\%_{abs}$  previously reported [22]. The n-MWT cells exhibit a lower FF than the n-Pasha cells, which stems from a higher series resistance. The major contributions to series resistance and FF losses are summarized in Table 4.

As can be seen in Table 4, the largest factor contributing to series resistance in n-MWT cells is the busbars, which deviate from the n-Pasha situation in that no tab is soldered to the busbar to enhance conductance. Resistive losses therefore occur in transport through the busbar to the vias. Several options exist for reducing the resistive losses and consequently the FF loss of n-MWT cells. A straightforward option is to increase the number of vias, which shortens both the busbars and the metal fingers at the same time; however, a drawback of this could be the increased chance of recombination and thus  $V_{\rm oc}$  loss as a result of the numerous contact points.

### n-MWT cells with new frontside patterns

To improve n-MWT performance, new MWT patterns with 36 vias (six rows, each with six vias) were designed. The simplest new n-MWT design was

Source of R <sub>series</sub> in MWT cell	<b>R</b> <sub>series</sub>	FF loss
Metal via resistance	$0.2 \text{m}\Omega$	0.3% <sub>abs</sub>
Front- and rear-side busbars	$0.7$ m $\Omega$	1.1% <sub>abs</sub>
Increase in $I_{\rm sc}$		0.1% <sub>abs</sub>
Total	$0.9 \text{m}\Omega$	1.5% <sub>abs</sub>

Table 4. Calculated contributions to series resistance and FF losses of n-MWT cells compared with n-Pasha cells.

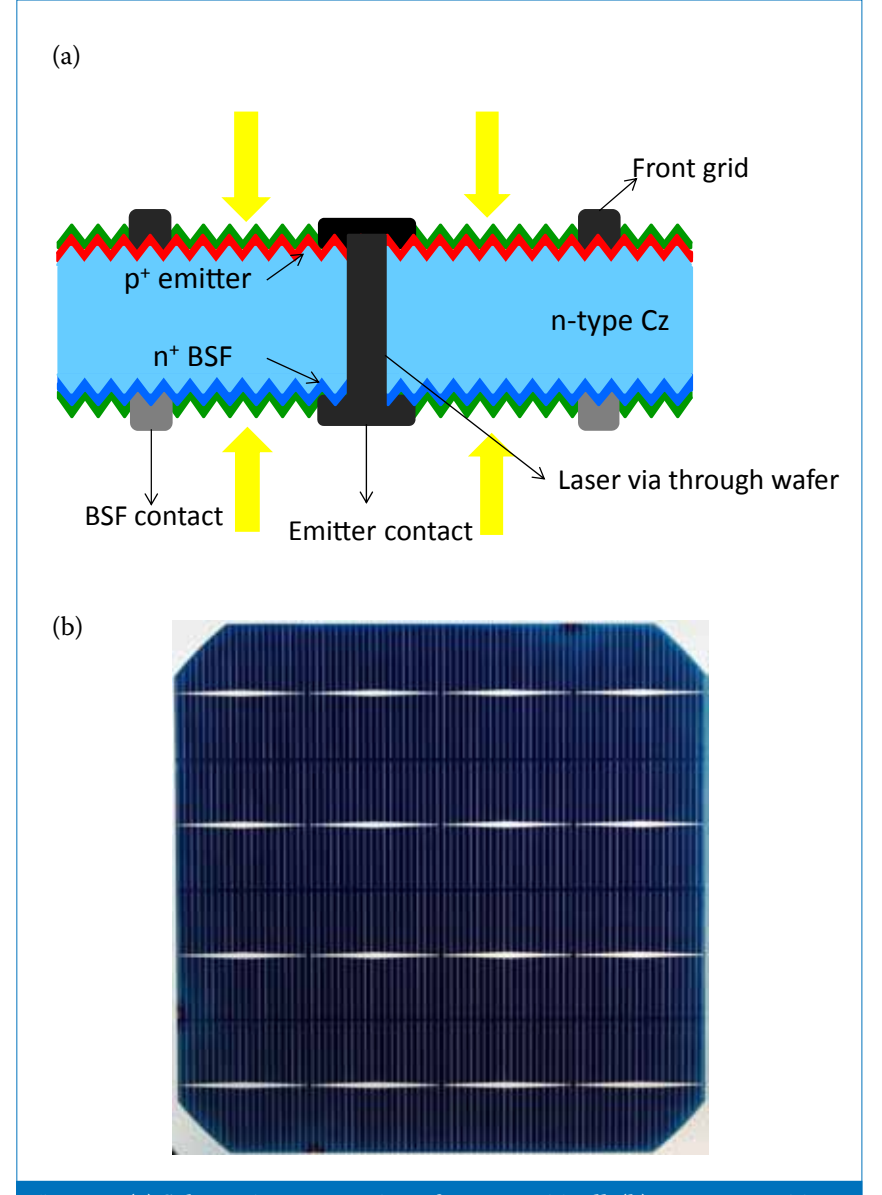


Figure 6. (a) Schematic cross section of an n-MWT cell; (b) a  $4\times4$  n-MWT front-grid design, with tapered busbars. The 16 vias are located in the thicker parts of the busbars. The metal fraction of the front-side metallization is around 5% of the total area.

based on six thin busbars connecting the rows of vias. The rear pattern also consists of thin busbars, connecting 7×7 (-4, because of semi-square wafer format) base contact points (Figs. 7(a) and (b)). Alternatively, different front-side patterns can be designed for improved aesthetics. Two examples were tested: the so-called 'starship' pattern and a circles pattern (Figs. 7(c) and 7(d)). All three 6×6 front-side configurations were combined with the rear-side metal pattern shown in Fig. 7(b) and compared with the 4×4 pattern in a cell experiment consisting of four groups.

The  $I_{\rm sc}$  and  $V_{\rm oc}$  data of the four groups are shown in Fig. 8; these two parameters were both found to depend mainly on the metal fraction. The increased number of vias did not

seem to have a negative effect on the passivation ( $V_{\rm oc}$ ) at this stage. The 'old'  $4\times4$  n-MWT pattern has the largest metal fraction of around 5% including the busbars, resulting in the lowest currents and voltages. The 'new' n-MWT pattern, with busbars and 36 vias, has the smallest metal fraction of 3.1%, which resulted in cells with an average high current of 9.63A, and an average  $V_{\rm oc}$  of 654mV.

"To improve n-MWT performance, new MWT patterns with 36 vias were designed."

As expected, the FF for the  $6\times6$  busbar pattern is clearly better than for

the 4×4 busbar pattern, but the highest FFs are obtained for the 6×6 starship pattern, which is specially modelled and designed to limit resistance losses (Fig. 9). The highest average efficiency of 20.3%, however, is obtained for the 6×6 busbar pattern because of its superior  $I_{\rm sc}$  and  $V_{\rm oc}$ .

Another important benefit of the 6×6 busbar pattern is that the paste consumption for both the front and the rear metallization is significantly reduced compared with that for the 4×4 pattern. The paste consumption for the latter is similar to that for three-busbar n-Pasha cells. In this experiment the reduction for the 6×6 pattern is already over 20%, and it is expected that in a (cost-)optimized situation a reduction of 50% should be possible, with only minor FF and

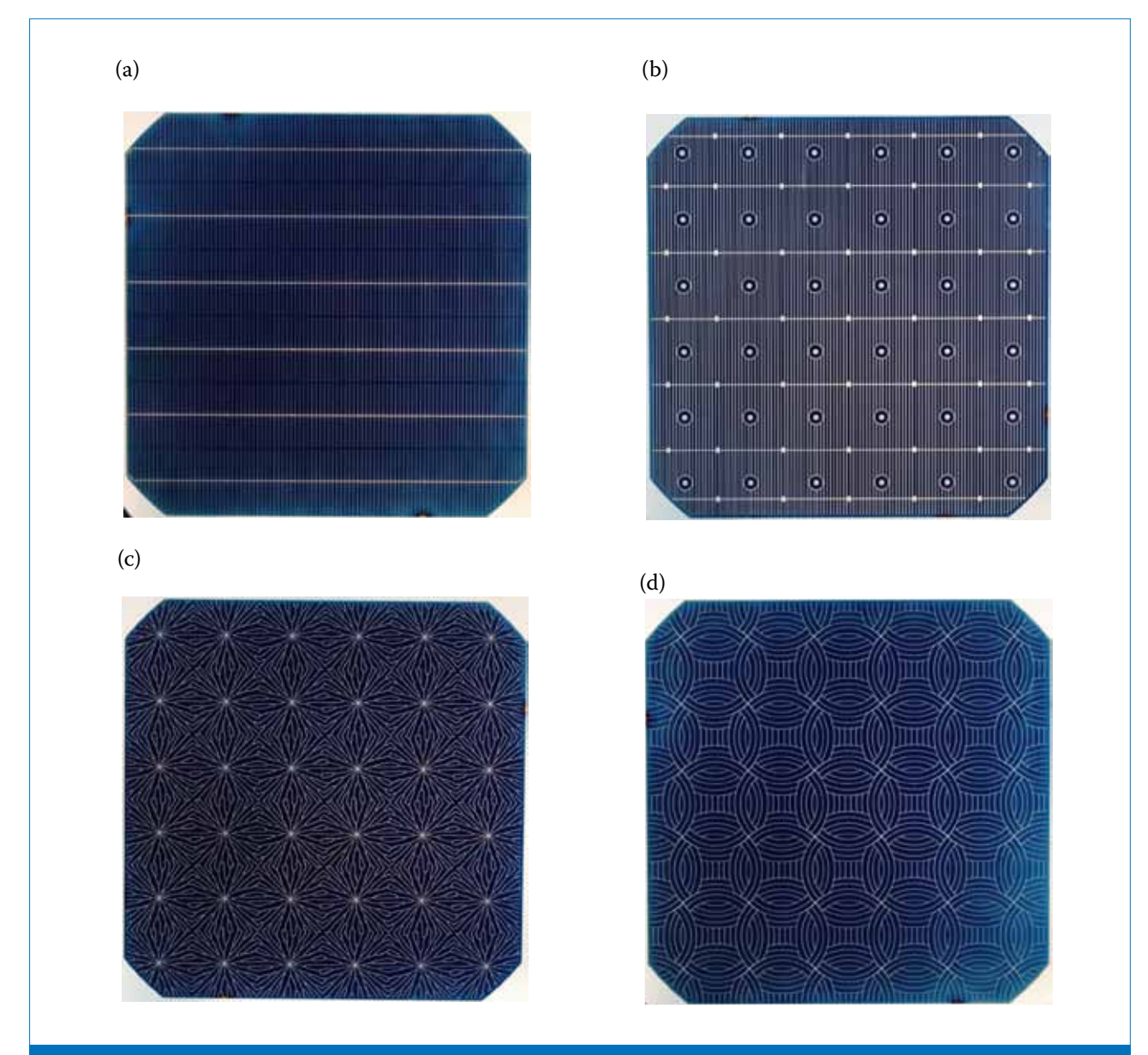


Figure 7. (a) Front-side 'new' n-MWT:  $6\times6$  vias with thin busbars; metal fraction  $\sim3.1\%$  of total cell area. (b) Rearside 'new' n-MWT:  $6\times6$  emitter contacts and  $(7\times7)-4$  base contacts (corners are excluded because of the semi-square wafer). (c) Starship pattern; metal fraction  $\sim4.7\%$  of total cell area. (d) Circles pattern; metal fraction  $\sim4.4\%$  of total cell area.

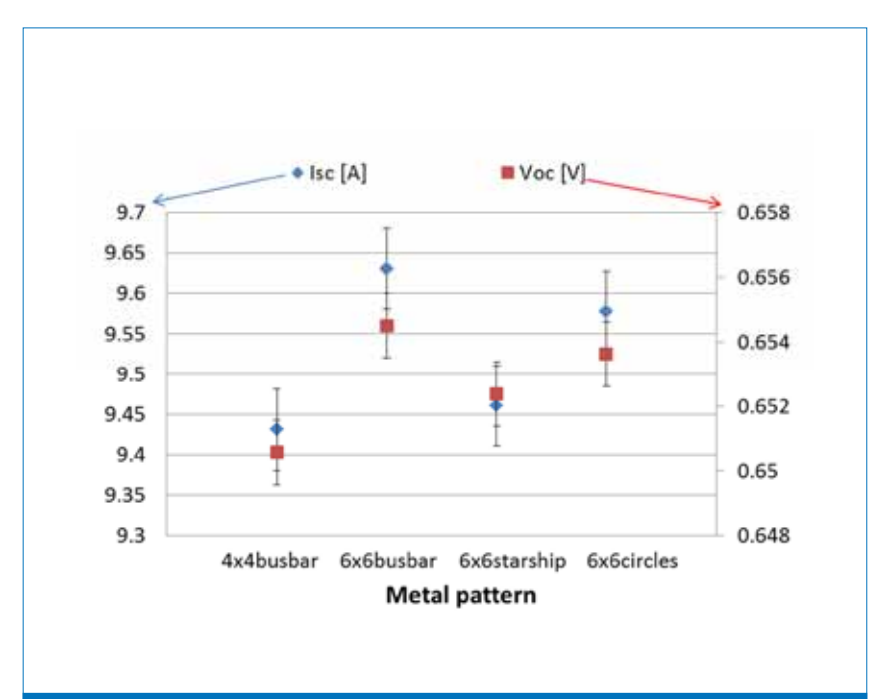


Figure 8.  $I_{\rm sc}$  and  $V_{\rm oc}$  of n-MWT cells with different numbers of vias (16 and 36) and different front metal patterns.

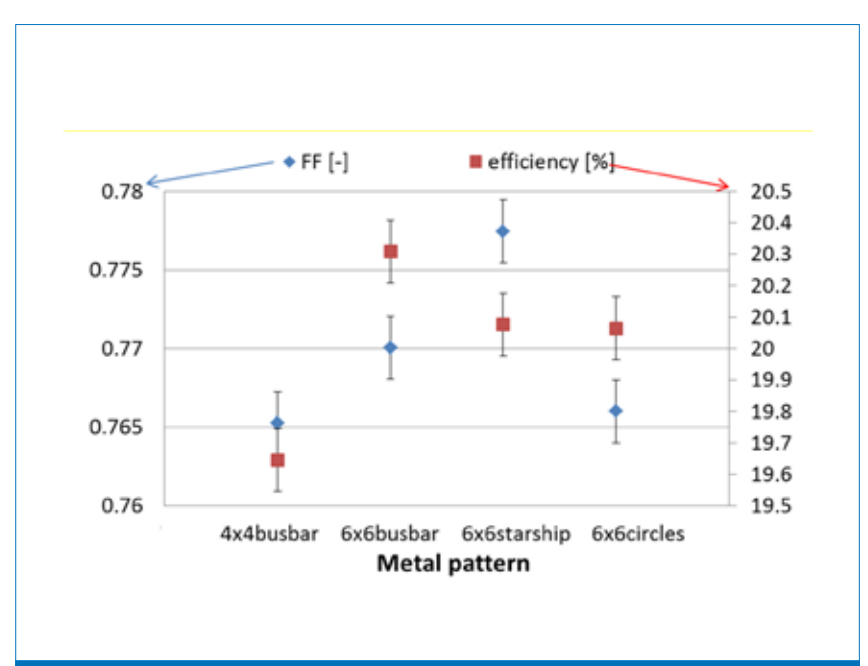


Figure 9. FF and efficiency of n-MWT cells with different numbers of vias (16 and 36) and different front metal patterns.

efficiency penalties.

### n-MWT modules

In two recent large n-MWT runs, high-quality n-Cz material and process improvements adopted from recent n-Pasha cell optimizations were used [23,24]. In the first run, the old via pattern with 4×4 vias was employed (see Fig. 6(b)). A best cell efficiency of 20.5% (certification pending) and average efficiencies over 60 cells of 20.3% were obtained. These cells were assembled in a 60-cell module using commercially available equipment

from Eurotron to pick and place the cells onto the copper backsheet foil [14]. The module has been tested using an A-class multi-flash solar simulator to demonstrate a power of 291Wp under STC, as can be seen in Fig. 10. The average cell data and module I-V are shown in Table 5.

In the second run, the best  $6\times6$  via pattern was used (see Fig. 7(a)); in addition, recent improvements from n-Pasha cells were transferred to the n-MWT cells. The results obtained from this run were a best cell efficiency of 21.0% (measured on a reflecting chuck) and an average

efficiency of 20.8% over more than 100 cells. The efficiency distribution of the full batch of 134 cells (shown in Fig. 11) was quite narrow, indicating a very stable process. The best 60 cells yielded an average 20.9% efficiency and will be assembled into a module in September 2014. With a CtM ratio similar to that for the 4×4 via module, a module power output of over 300W is expected.

### **Summary and conclusions**

Two n-type solar cell and module concepts have been discussed: the n-Pasha solar cell and bifacial module, and the n-MWT cell and module. In the case of n-Pasha cells, recent developments involve improved stencil-printed metallization, resulting in an increased  $I_{\rm sc}$  and  $V_{\rm oc}$ and efficiencies of up to 20.5%. For the bifacial module aspect, research has been done on improving the module output power by changing the albedo. A gain of  $20\%_{\rm rel}$  in module output power was obtained with optimized background, increasing the module power from 314W to 376W. Furthermore, a new bifacial module concept called Bumblebi was introduced, in which the front and rear response (and appearance) of the modules are equalized. Equal front and rear responses will be especially useful if the bifacial modules are used in an east-west orientation, because in this case the harvested power will be more evenly distributed over the whole day.

"A module under construction using sixty n-MWT cells with an average efficiency of 20.9% is expected to deliver a power output of over 300W."

For n-MWT cells, the front-side metallization pattern has been changed significantly by adopting 36 (6×6) vias instead of the 16 (4×4) that have traditionally been used up to now. This results in reduced lengths of busbars and fingers and consequently an increase in FF. The metal coverage on the front side was reduced from 5% to 3% of the total area, resulting in a gain in  $I_{\rm sc}$  and  $V_{\rm oc}$ , and at the same time a significant reduction in Ag consumption. All these factors will result in a (much) lower cost/Wp. For the improved n-MWT design, average efficiencies of 20.8% over a large batch (134) of cells have been obtained, with

manufacturing the n-MWT cells and Cell

**Processing** 

the highest recorded efficiencies being 21% (before mismatch correction). The pattern of the backsheet for the modules was adjusted accordingly. A module under construction (September 2014) using sixty n-MWT cells with an average efficiency of 20.9% is expected to deliver a power output of over 300W.

### Acknowledgements

The authors are grateful for the collaboration with our research

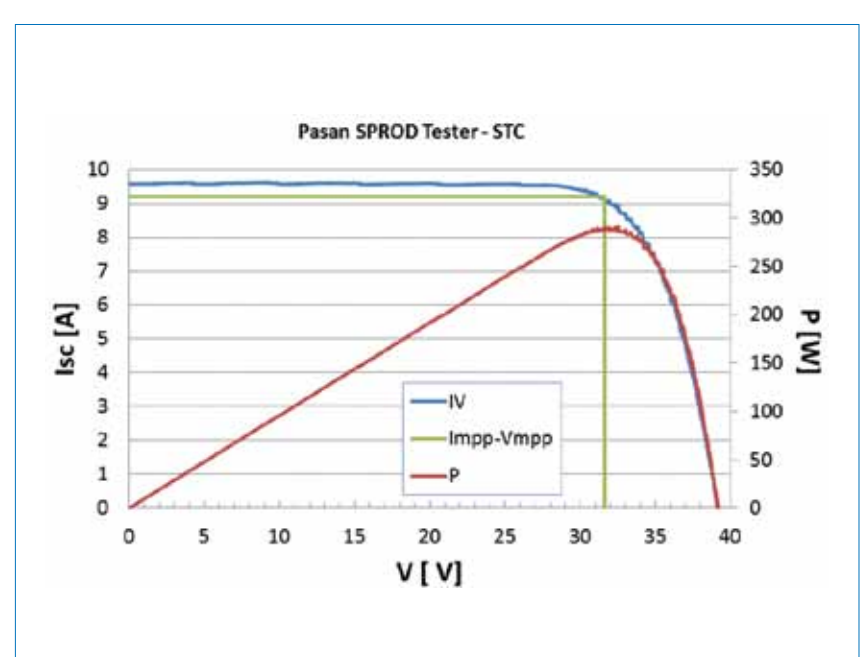


Figure 10. I-V data for a 60-cell module made with n-MWT cells with 4×4 vias. A resulting power of 291Wp was demonstrated.

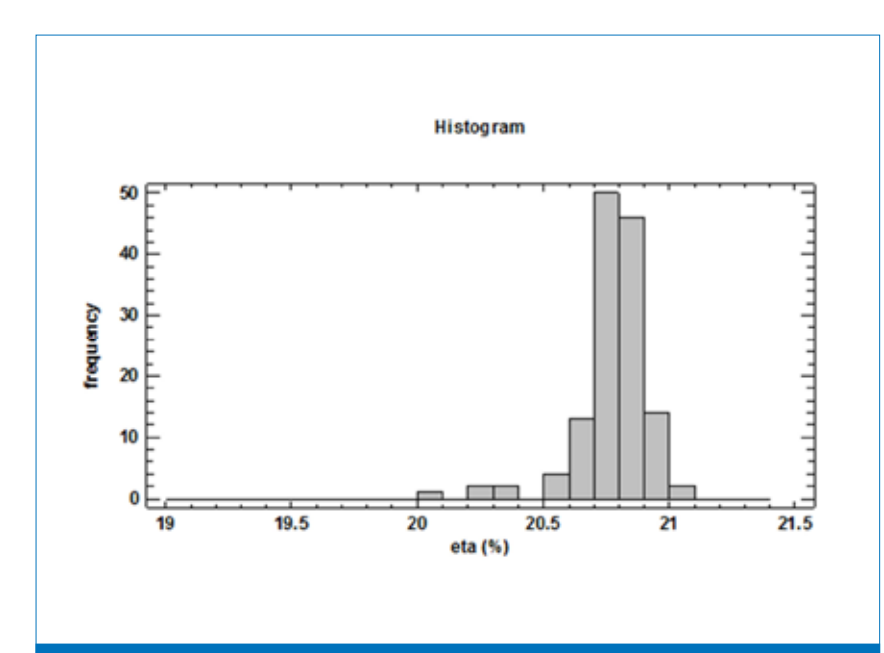


Figure 11. Efficiency distribution of 134 n-MWT cells fabricated with the optimized 6×6 via pattern and including recent n-Pasha improvements. The highest efficiency obtained was 21%.

#### References

modules.

[1] SEMI PV Group Europe 2014, "International technology roadmap for photovoltaic (ITRVP): Results 2013", 5th edn (March) [available online at http://www.itrpv.net/Reports/ Downloads/].

partners from the TKI [25] projects

NChanted and Pamplona, and in

particular to the companies Tempress

and Eurotron for their help in

- [2] Glunz, S. et al. 1998, Proc. 2nd WCPEC, Vienna, Austria, p. 1343.
- [3] Macdonald, D. & Geerligs, L.J. 2008, Appl. Phys. Lett., Vol. 92, p. 4061.
- [4] SunPower [http://us.sunpower. com/].
- [5] Panasonic 2014, "Panasonic HIT" solar cell achieves world's highest energy conversion efficiency of 25.6% at research level", Press Release (April) [http://eu-solar. panasonic.net/fileadmin/user\_ upload/News\_PDFs/140410\_ Panasonic\_HIT\_E.pdf].
- [6] Song, D. et al. 2012, Proc. 38th IEEE PVSC, Austin, Texas, USA.
- Gonsui, S. et al. 2013, Proc. 28th EU PVSEC, Paris, France.
- Hsieh, P. et al. 2013, Proc. 28th EU PVSEC, Paris, France.
- [9] Boescke, T.S. et al. 2012, Proc. 38th IEEE PVSC, Austin, Texas, USA.
- [10] Lanterne, A. et al. 2014, Proc. 4th SiliconPV, 's-Hertogenbosch, The Netherlands.
- [11] Fraunhofer ISE 2013, "24 percent efficient n-type silicon solar cell - Top-notch European research raises potential for cost reductions in photovoltaics", Press Release (November) [http:// www.ise.fraunhofer.de/en/ press-and-media/press-releases/ presseinformationen-2013/24prozent-siliciumsolarzelle-auf-ntyp-material].
- [12] Romijn, I.G., Fang, L. & Vlooswijk, A. 2012, Photovoltaics International, 15th edn, p. 81.
- [13] Burgers, A.R. et al. 2011, Proc. 26th EU PVSEC, Hamburg, Germany.
- [14] Bennet, I.J. et al. 2009, Proc. 24th

	T <sub>m</sub> [°C]	Irr [W/m²]	I <sub>sc</sub> [A]	<i>V</i> <sub>oc</sub> [V]	<i>P</i> <sub>m</sub> [W]	FF [%]	Cell eff [%]
Cell average			9.51	38.927	290.79	78.50	20.28
B392 (8 flashes)	26.2	1000	9.59	39.196	290.99	77.42	20.29
Rel. CtM ratio change			+0.81%	+0.69%	+0.07%	-1.41%	

Table 5. Average cell and module I-V data for a 60-cell module made with n-MWT cells with  $4\times4$  vias.

- EU PVSEC, Hamburg, Germany.
- [15] Guillevin, N. et al. 2014, Proc. 8th SNEC Intl. PV Power Gen. Conf., Shanghai, China.
- [16] Energy Matters 2014, "Yingli Solar trialing n-MWT manufacturing technology", News Report [http://www.energymatters.com.au/index.php?main\_page=news\_article&article\_id=4315].
- [17] Cesar, I. et al. 2014, *Proc. 4th SiliconPV*, 's-Hertogenbosch, The Netherlands.
- [18] Romijn, I.G. et al. 2013, *Photovoltaics International*, 20th edn, p. 44.
- [19] Mishima, T. et al. 2011, Solar Energy Mater. & Solar Cells, Vol. 95, pp. 18–21.
- [20] Kreinin, L. et al. 2011, *Proc. 26th EU PVSEC*, Hamburg, Germany.
- [21] van Aken, B. & Carr, A. 2014, Proc. 40th IEEE PVSC, Denver, Colorado, USA.
- [22] Guillevin, N. et al. 2011, Proc. 26th EU PVSEC, Hamburg, Germany.
- [23] Romijn, I.G. et al. 2014, Proc. 8th SNEC Intl. PV Power Gen. Conf., Shanghai, China.
- [24] van de Loo, B. et al. 2014, *Photovoltaics International*, 24th edn, p. 43.
- [25] TKI Solar Energy [http://www.tkisolarenergy.nl/]

### **About the Authors**



Ingrid Romijn joined ECN Solar Energy in 2004, where she started working as a researcher and later on (2006) as a project leader in the

crystalline silicon group. Research topics included passivating layers, optimization of  $\mathrm{SiN_x}$  deposition systems and (advanced) p-type solar cell concepts. During 2011 the focus of her work shifted towards the development and industrialization of n-type cell concepts. In 2012 Ingrid became the topic coordinator for industrial n-type cells and modules at ECN Solar Energy.

Bas van Aken studied materials science at Delft University of Technology, after which he studied for his Ph.D. at the University of Groningen. Following that he worked as a postdoctoral researcher at Cambridge University and at the Max Born Institute for Nonlinear and Ultrafast Optics in Berlin. After around five years in the thin-film Si group at ECN Solar Energy, he is now with the PV modules and application group, where he focuses on the fabrication and reliability of n-type PV modules – both conventional H-pattern modules and more advanced concepts, such as backcontact technology and bifacial modules.



Ian Bennet is a researcher at ECN Solar Energy and received a Ph.D. in materials science from the University of Bath. He has worked for

several research institutes, investigating high-temperature processing of ceramic materials. Ian has been with ECN since 2006 as a member of the module technology and application group, where he has been involved in the development of module technology for back-contact cells and the application of new and novel module materials and module concepts.

LJ (Bart) Geerligs has been at ECN Solar Energy since 2000, where he has set up several research fields. From 2004 he led a number of projects in which n-type cell technology at ECN was developed. From 2009 to 2010 he was project leader at ECN for the development and successful transfer to industrial pilot production of n-Pasha cell technology (subsequently transferred to mass production), and from 2010 to 2012 for the development and successful transfer to industrial pilot production of n-MWT cell technology. Since 2012 he has been the coordinator of R&D at ECN for highefficiency silicon cells and applications of nanotechnology, and the coordinator of a European project on reducing the environmental footprint of silicon PV, including design for recycling.



Nicolas Guillevin is a researcher in the device architecture and integration group at ECN Solar Energy. He joined ECN in 2007, where he

started his research activities in the development of n-type-based silicon solar cells, focusing mainly on back-contact cell architectures (EWT, MWT and IBC). Nicolas studied at the National Engineering School of

Industrial Ceramics in Limoges (France), where he obtained a master's in the field of materials science and processes.

Astrid Gutjahr studied mineralogy at the University of Bonn and was a postdoctoral researcher in the liquid phase epitaxy group at Max Planck Institute for Solid State Research in Stuttgart. In 1999 she joined ECN, where she has worked on the development of RGS, a crystalline Si ribbon growth technology. Astrid's current research focuses on the characterization and cell processing of n-type silicon wafer material.

Eric Kossen has been working in the solar department at ECN Solar Energy as a senior process engineer for 17 years. He specializes in different metallization concepts for n- and p-type solar cells, especially in fine-line stencil printing. Eric also has wide experience in delivering training on the subject of metallization to engineers and operators in industry.



Martien Koppes began working as a chemist in the molten carbonate fuel cell group at ECN Solar Energy 23 years ago. For the last 14 years

he has been a researcher in solar energy. Martien's main work concerns the chemical aspect of solar cells, with a focus on etching and cleaning.

Kees Tool has been working in the solar energy field for almost 20 years. After an education in chemistry, he embarked on a career in solar energy as a researcher. For around seven years his main work has involved transferring both n-type and p-type ECN technology to industry. He also carries out troubleshooting and tuning of industrial crystalline silicon solar cell production lines.

### **Enquiries**

Ingrid Romijn ECN Solar Energy P.O. Box 1 NL-1755 ZG Petten The Netherlands

Tel: +31 224 56 4959 Fax: +31 224 56 8214 Email: romijn@ecn.nl